Experimental Verification of Spliced Buckling Restrained Braces

KENNETH T. TAM, RONALD L. MAYES, DAVID L. MCCORMICK, ANINDYA DUTTA and CRAIG B. GOINGS

ABSTRACT

A critical facility constructed in the 1980s was housed in a building whose original seismic force-resisting system included chevron-braced frames and pre-Northridge earthquake moment frames. In the mid-1990s, a code-based seismic retrofit was designed. This phased retrofit was only partially completed. A more recent seismic evaluation of the building in its partially retrofitted condition revealed major structural deficiencies. Another retrofit was designed using field-spliced buckling restrained braces (BRBs) that allowed the building to remain operational during construction. The paper summarizes the analyses performed for the seismic retrofit and the development, prototype testing and erection of the spliced BRBs. The project testing protocol was compared with current AISC *Seismic Provisions*' testing protocol for BRBs (AISC 341-10), which shows that if properly detailed and fabricated, BRBs used for this retrofit project can have peak and cumulative ductility well in excess of the current AISC testing criteria.

Keywords: seismic retrofit, buckling restrained braces, field-splice details.

INTRODUCTION

A critical facility constructed in the 1980s was housed in a building whose original, seismic force-resisting system includes chevron-braced frames in the long direction and pre-Northridge earthquake moment frames in the short direction. In the mid-1990s, a code-based seismic retrofit was designed. This retrofit, which was scheduled to be completed in phases, was only partially completed after approximately 12 years. A seismic evaluation of the building in 2008 in its partially retrofitted condition revealed major structural deficiencies.

Consequently, a seismic retrofit that consisted of a combination of exterior buttresses with buckling restrained braces (BRBs) and BRB frames at some interior locations was developed. One of the major design constraints was that the facility needed to remain operational during the construction with minimal disruption to existing process utilities.

During the design phase, concern was expressed about the maneuverability of the BRBs in tight spaces inside the building. This resulted in the development of a field-splice detail for the BRBs, which permitted erection of the braces in half-segments. Because splicing of BRBs had not been performed previously, the supplier was required to demonstrate similar performance to the un-spliced BRBs through prototype testing. After the testing, the spliced BRBs were successfully installed and the project was completed with minimal disruption to the operations of the facility.

A summary is presented of the analyses performed for the seismic retrofit and the development, prototype testing and erection of the spliced BRBs. The project testing protocol was compared with current AISC testing protocol for BRBs (AISC 341-10; AISC, 2010), which shows that, if properly detailed and fabricated, BRBs used for this retrofit project can have peak and cumulative ductility well in excess of the current AISC testing requirement.

The subject building is located in South San Francisco, California, and was built circa 1980. It is two stories with a rectangular plan (100 ft by 364 ft). The original building's seismic force-resisting system includes braced frames in the long direction and pre-Northridge earthquake moment frames in the short direction. Figure 1 shows an aerial view of the building. In the mid-1990s, a seismic retrofit was designed to the requirements of the 1991 Uniform Building Code (UBC) with an importance factor of $I = 2.5$. The retrofit primarily involved the addition of braced frames and augmentation of existing moment frame connections at the roof level with haunches. The retrofit, which was progressing in phases during the yearly shutdowns, was only partially (about 60%) completed in 2008 when a new seismic evaluation of the building was commissioned. Major deficiencies in the structure in its partially retrofitted condition were identified. Consequently, a retrofit design was undertaken.

Kenneth T. Tam, S.E., Senior Project Manager, Simpson Gumpertz & Heger, Inc., San Francisco, CA (corresponding). Email: kttam@sgh.com

Ronald L. Mayes, Ph.D., Staff Consultant, Simpson Gumpertz & Heger, Inc., San Francisco, CA. Email: rlmayes@sgh.com

David L. McCormick, S.E., Senior Principal, Simpson Gumpertz & Heger, Inc., San Francisco, CA. Email: dlmccormick@sgh.com

Anindya Dutta, Ph.D., S.E., Senior Project Manager, Simpson Gumpertz & Heger, Inc., San Francisco, CA. Email: adutta@sgh.com

Craig B. Goings, S.E., P.E., Associate Principal, Simpson Gumpertz & Heger, Inc., San Franciso, CA. Email: cbgoings@sgh.com

Many of the spaces are extremely congested with process piping, mechanical ducts and other equipment. Most of the processes could not be altered or taken out of service, even temporarily. Furthermore, two buildings exist adjacent to the north elevation with minimal seismic separation, and a large multilevel pipe rack exists along most of the length at the south elevation. Given the site constraints, a retrofit scheme was developed that utilized exterior steel buttresses on the south elevation, connected to the building with horizontal BRBs at the floor and roof levels, and added BRBs within some of the frame lines that were accessible.

SEISMIC DEFICIENCIES

The partially retrofitted building was analyzed, and the following deficiencies in the seismic load resisting system were identified.

Pre-Northridge Moment Frames

The original lateral system in the transverse direction of the building comprises of W24 (roof) and W30 (second floor) wide flange beams connected to W14 columns with typical pre-Northridge moment connections (WUF) that are susceptible to brittle failure. The frames also have weak panel zones that have capacities well below that required to develop yielding of the beam.

Chevron-Braced Bays

All of the original braced frames and a majority of the retrofitted braced frames have a chevron configuration with beams that were not sized to carry the unbalanced force. This is worsened by the fact that the original braced frames consist of double-tiered chevron frames (two levels of chevron frames per story), where the intermediate beam between story levels consists of W10 wind girts that were oriented with the strong axis in the horizontal position.

Inadequate Brace Connections

All the braces in the original building, as well as a majority of the retrofitted braces and their connections, were not detailed to develop the strength of the braces.

Close Proximity of Adjacent Buildings and Propensity for Pounding

The subject building is located in a congested building complex with at least two buildings spaced closely enough to cause a pounding hazard (see Figure 2).

Other Issues

The building also has a relatively weak, bare-metal roof diaphragm, as well as inadequate collectors and collector connections, in part due to the fact that the retrofit from the 1990s was not completed.

Fig. 1. Aerial view of the facility showing the subject building.

RETROFIT ANALYSIS

A code-type analysis using an *R* factor was not adequate to account for the differing behavior of the various lateral systems that were built in different periods of time. Therefore, a performance-based design approach outlined in ASCE 41-06, *Standard for Seismic Rehabilitation of Existing Buildings* (2006), was followed. The performance objective is to exceed life safety under the BSE-1 level earthquake and collapse prevention under the BSE-2 level earthquake. A nonlinear dynamic analysis using ASCE 41-06 was performed. The analysis was iterative in that it was first required to conceive retrofit concepts and introduce them into the 3D model and then validate through the dynamic analysis that they alter the behavior of the structure in a way that was anticipated. The owner next provides input regarding acceptability with regards to operations and cost. The scheme was then incrementally modified until a cost-effective scheme with little or no temporary or permanent effect on operations was developed.

Retrofit concepts including dampers and conventional braced frames were considered, but it was soon determined that BRBs provided the best protection for the existing braced frames and their connections and limited the drifts in the direction of the moment frames to protect the weak connections and to minimize pounding. Through strategic placement of BRBs—which required replacement of existing chevron braces at some locations—diaphragm strengthening was limited to local areas, and only a limited amount of collector strengthening was required.

As the design progressed, the contractor expressed concerns about maneuverability of the BRBs (approximately 40 ft long) inside the congested building. A field-splice detail for the BRBs, allowing transport of the braces in half-segments, was developed. Because of concerns regarding alignment of the spliced segments, the vendor was required to demonstrate through prototype testing that the spliced braces would perform as well as the non-spliced BRBs. The BRBs were tested at the NCREE facility in Taiwan and the results compared to the analytical model.

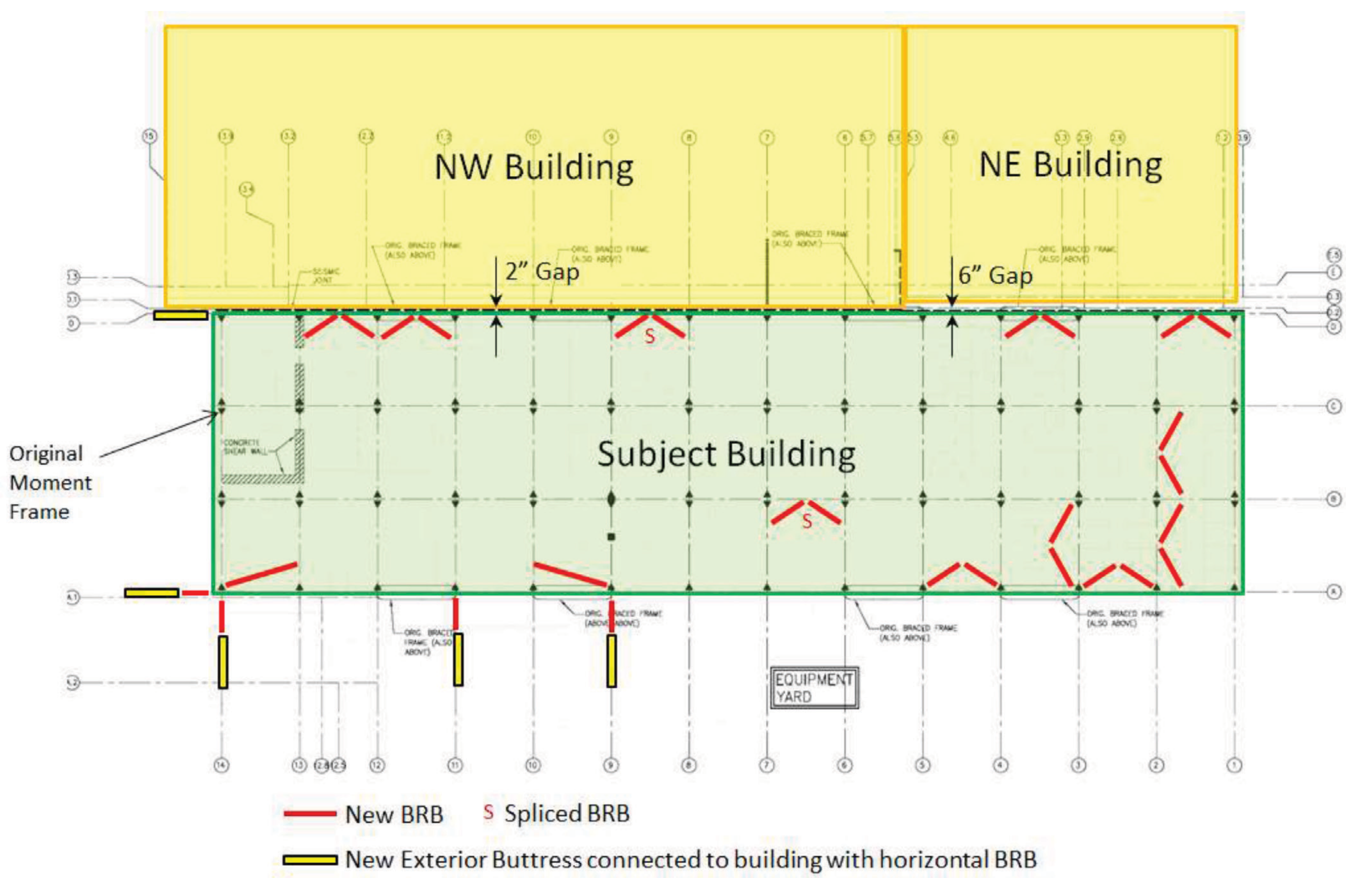

Fig. 2. Plan showing proximity of adjacent buildings.

Table 1. Acceptance Criteria for BRB			
Shaking Level	Performance Goal	Average of 7 Time Histories	Maximum of 7 Time Histories
BSE-1	Life safety	$8\Delta_{by}$	$12\Delta_{by}$
BSE-2	Collapse prevention	$12\Delta_{by}$	$18\Delta_{by}$

Ground Motion for Nonlinear Analysis

A suite of seven ground motions was used for the nonlinear time-history analyses. These ground motions were scaled to a site-specific spectra generated using the next-generation attenuation (NGA) relationships. As the soil profile changes dramatically under the building, the worst-case ground motions associated with a firm and soft soil site were used.

Nonlinear Analysis Model

A nonlinear finite element model of the lateral-load systems of the building was created using the analysis program CSI Perform. Existing double-angle and tube steel braces were modeled using backbone parameters from ASCE 41-06. One of the most important criteria for modeling the braces was to capture the behavior of weak connections. Where strength of the connection governed, a drastic drop in strength was incorporated into the model. The brace was considered ineffective after the connection fails. Similar modeling was performed to recognize substantial loss of strength when the braces buckled. The moment frames were modeled with a nonlinear panel zone spring to capture the effects of the weak panel zone.

The effects of foundation flexibility were included into the model through the use of nonlinear elastic springs representing the passive and frictional resistance of the footings against the supporting soil. Nonlinear gap elements with compression only stiffness were used to capture foundation uplift. The upper- and lower-bound analysis of the structure using 150% and 67% of the soil stiffness to capture the variability in the behavior were used in accordance with the requirements of ASCE 41-06.

The BRBs were modeled with a component consisting of stiff end zones and a yielding core. The backbone parameters are shown in Figure 3. These parameters were based on prior testing performed by the BRB manufacturer. Because there are no criteria for checking BRBs in ASCE 41-06, strains in the individual BRBs were checked to the criteria listed in Table 1. These criteria were derived based on a review of existing test data from the BRB manufacturer. It can be seen from Table 1 that separate criteria for the average of the seven time histories and maximum from any single event were used. Both criteria needed to be satisfied.

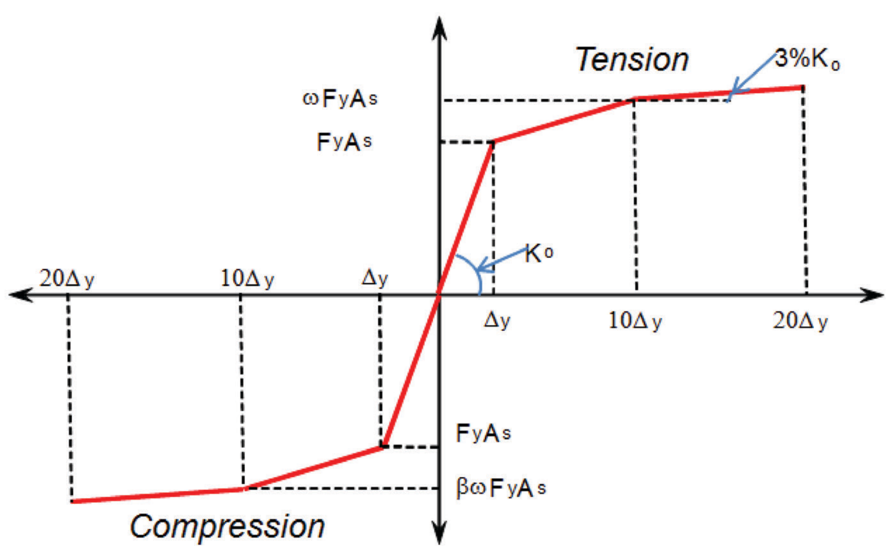

Fig. 3. Backbone properties of buckling restrained braces.

DETAILS OF THE SPLICED BRB

As indicated previously, a spliced BRB was developed to help with the maneuverability of the BRB members within congested areas. The spliced BRB consists of two BRB segments; each segment alone is similar to a standard BRB consisting of a yielding core, transition zones and nonyielding end zones (see Figure 4). The concept behind the spliced BRB is that the splice zone is designed to remain elastic (similar to typical end zones). The core at the splice zone has a cross-sectional area much larger than the yielding core, and the splice of the casing was designed to have flexural stiffness exceeding the casing along the remaining length of the BRB. Several conceptual splices were assessed, including welded and bolted options (see Figure 5).

The welded option was chosen based on the stability of the cruciform shape as well as the constructability of the detail. The final detail consists of cruciform cores at the splice zone, which are connected with full-penetration welds. The outer casing was connected with plates welded to each other and to the casing with fillet welds. The final detail of the splice is shown in Figure 6.

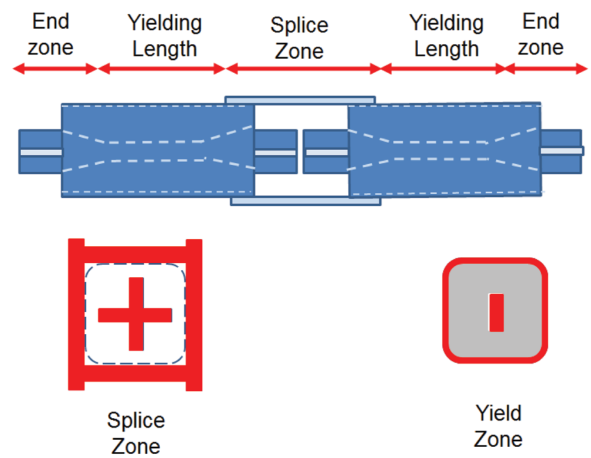

Fig. 4. Conceptual sketch for spliced BRB.

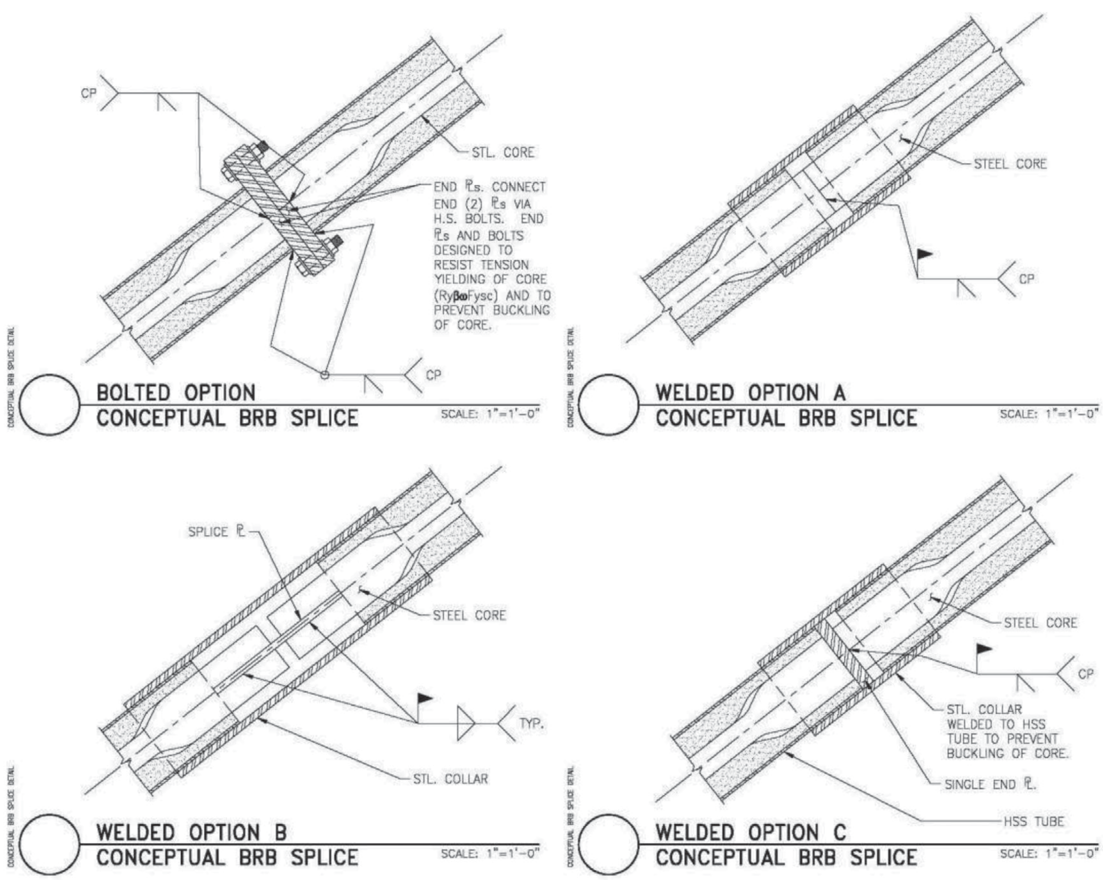

Fig. 5. Conceptual studies of splice options.

Note that the yielding core of the spliced BRB is shorter than a standard BRB of the same length because there are essentially four end and transition zones, doubling that of a standard BRB. The analysis model included this to capture the correct load distribution within the structure as well as the ductility demand on the cores. Locations of the spliced BRB within the structure were closely coordinated with the contractor during the design phase. Many site visits and some inspection openings were made during the design phase to work out the locations of the spliced and nonspliced BRBs. Subsequently, many iterations of the model were created.

BRB PROTOTYPE TESTING

Because spliced BRBs have not been implemented before, prototype specimens were fabricated for testing. The objectives of the testing program were as follows:

- To validate that the spliced BRB is feasible and the behavior is as anticipated.
- To determine any potential obstacles related to the erection of the spliced BRBs.
- To ensure that the two halves of the spliced BRB can be properly aligned given the congested field conditions.

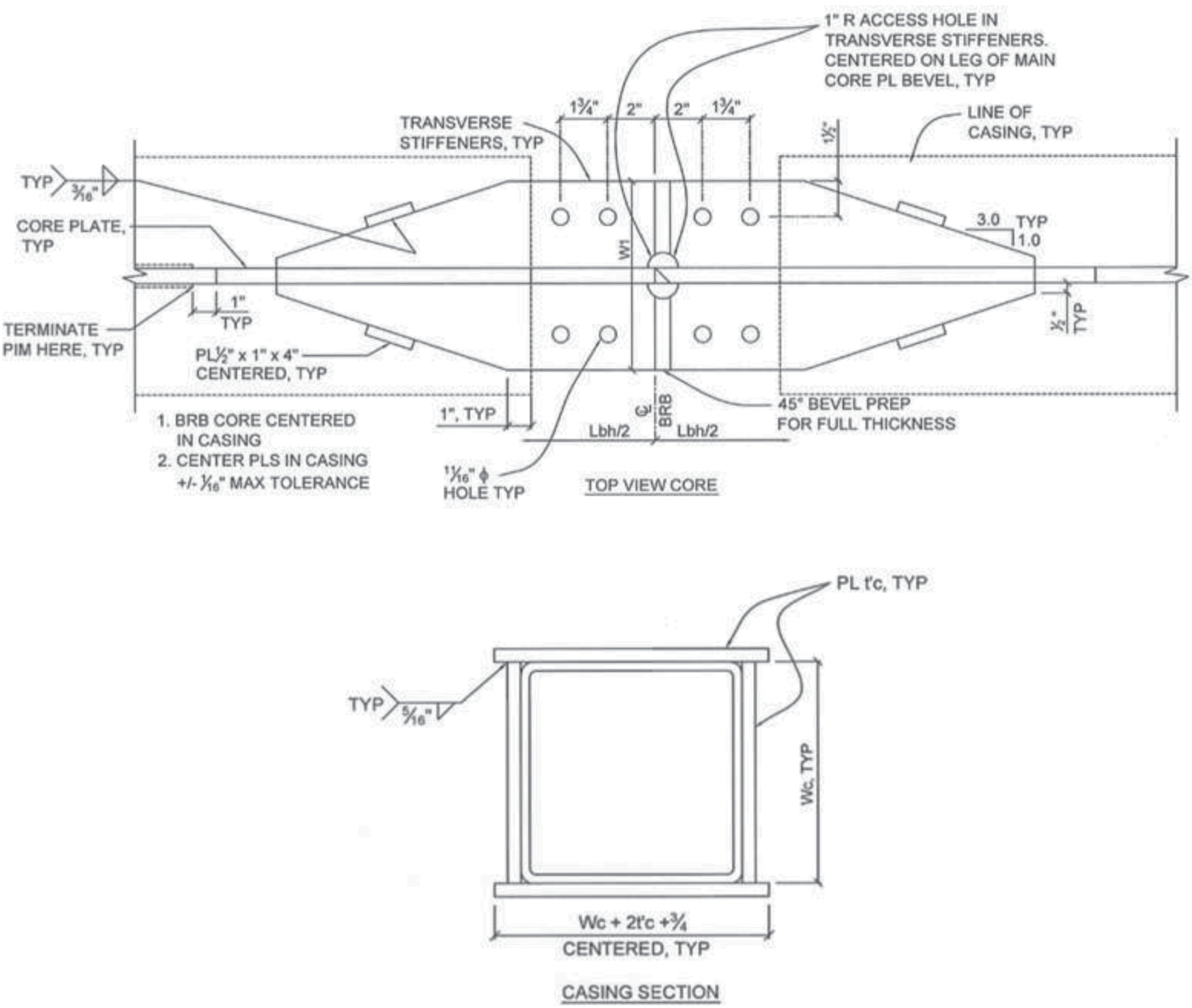

Fig. 6. Final details of splice.

Table 2. Summary of BRB Test Specimens							
Number	ID	Length, L_b (ft)	Yield Length, L_y (in.)	Casing Size	End Connections	P_{ysc} (kips)	Spliced
1	1901A1	12	86.2	HSS10×¼	Pin-end	250	No
2	1901A2	12	86.2	HSS10×¼	Pin-end	250	No
3	1902A1	21	125.6	HSS10×10×½	Bolted-end	230	Yes
4	1902A2	21	125.6	HSS10×10×½	Bolted-end	230	Yes
5	1903A	31	236.7	HSS10×10×½	Bolted-end	250	Yes
6	1904A	31	268.5	HSS10×10×½	Bolted-end	250	No

- To develop quality assurance requirements for splicing BRBs in the field.

Additionally, testing on three unspliced BRBs was performed to study the effects of the following:

- Performance of pin-ended BRBs with casing fabricated with circular HSS section. The pin-ended BRB was developed to be a high-performance brace that includes some of the special detailing not used in previous versions. Thus, testing was performed to validate the performance.

- Performance of relatively long and slender BRBs. Note that this was also intended to be a control, or comparison, to the spliced version.

DESCRIPTION OF PROTOTYPE SPECIMENS

A total of six specimens were tested. The yielding cores of the BRB were fabricated with ASTM A36 plate stock with the following properties: F_y = 41.9 ksi and F_u = 71.6 ksi based on average of two coupon tests using the 0.02% offset method. The gusset plates were made with ASTM A572 Grade 50 steel.

Three specimens were spliced. Two of the spliced specimens were 21 ft long and the third was 31 ft long. Three specimens were not spliced: two 12-ft-long pin-ended specimens, and one 31-ft-long bolted-end specimen. Properties of the test specimens are summarized in Table 2.

DESCRIPTION OF FABRICATION

The prototypes were fabricated at the manufacturing facility in Utah. The construction of the spliced specimens (specimens 3, 4 and 5) was observed to develop procedures to perform the splices and to identify potential problems during construction.

Method of Alignment

One of the objectives of the prototype testing was to determine whether the two halves could be properly aligned in the field. Alignment plates to align the cruciform cores were proposed (see Figures 7 and 8). The alignment plates were removed in stages as the cores were welded together. To align the casing, two pairs of steel angles were clamped onto the steel casings. A small amount of welding was used to connect the angles with the casing (see Figure 9). The alignment angles were removed in stages as the casing splice plates were welded. Figure 10 shows the finished spliced condition.

The original intent was to make the splice in the horizontal position (on the ground) prior to lifting the BRB into the final locations. However, it was determined that this required substantially more floor area than is available in the building. During one of our visits to the site during the design phase, the contractor requested the option of lifting each half of the BRBs into the inclined position (final position of the brace) prior to performing the splice. In order to replicate the actual condition of the site, one of the specimens was spliced in the inclined location (see Figure 11). As shown in Figure 11, the prototype was supported at the splice point by a crane. In the field, this would be accomplished by a combination of chains and come-alongs. The alignment, welding of the cores and welding of the casing plates of the specimen were performed in this position.

Effects of Welding of the Core

The cores were spliced with prequalified, full-penetration welds. The weld of the core splice was treated as a demand-critical weld with associated quality assurance (ultrasonic testing, magnetic particle testing) even though no yielding is expected to occur at this location. The maximum thickness of the core plates was 1 in. Some amount of distortion was observed, primarily due to the heat generated during the welding process. As a result, some out-of-straightness was measured after the cores were welded. It was noted that the sequence of laying down the weld beads was an important aspect of controlling the amount of distortion (i.e., the welder needed to alternate the weld placed on each leg of the cruciform core). Additionally, in order to prevent initial stressing of the core due to heating and subsequent cooling of the core, tightening of bolts at the end connections was permitted only after the splice was complete and adequate time passed for cooling of the welded zone.

Tolerance

As discussed earlier, the cores were aligned using alignment plates. Following this procedure, the out-of-plane offset tolerance of the cores was limited to 1/16 in. The out-of-straightness tolerance (both in-plane of the core and out-of-plane of the core, see Figure 12) was initially set to be 1/16 in. over the length of the completed brace. This was measured prior to welding of the cores. As part of the field quality assurance, a second measurement was required after the cores were welded. For this measurement, the tolerance was relaxed to 1/8 in. over the length of the brace. It was noted that during the welding of the splice of specimen 5, the out-of-straightness tolerance was exceeded in the out-of-plane direction. The measured out-of-straightness in the specimen was 1/4 in. over the length of the brace. This was likely due to sequence of laying down the weld beads. In lieu of attempting to straighten this specimen, it was decided to test the specimen to study the effect on performance of some

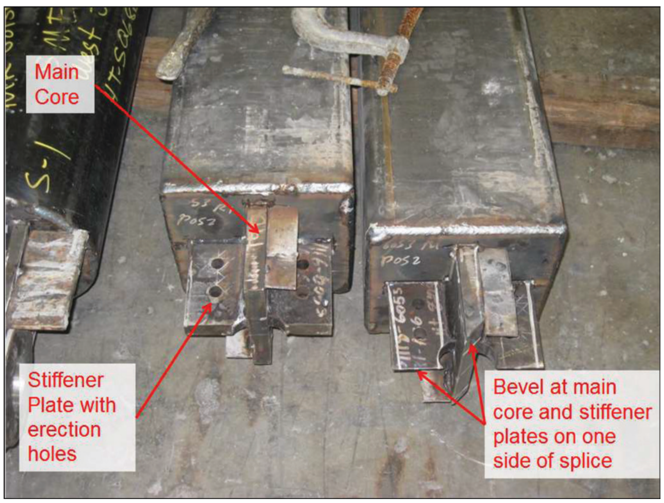

Fig. 7. Core at splice location.

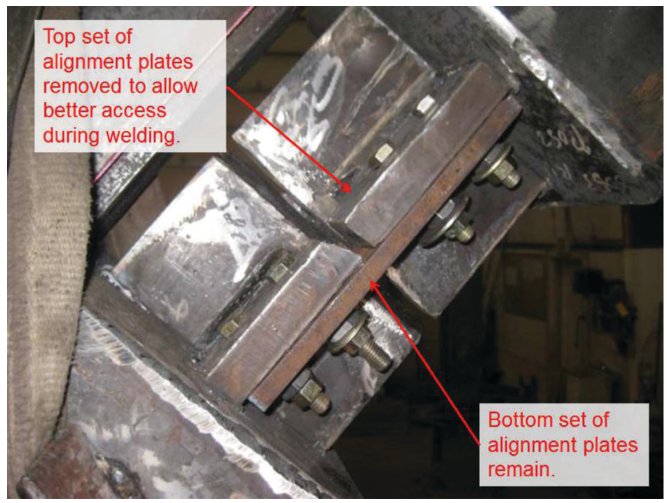

Fig. 8. Alignment plates at core at splice.

Fig. 9. Alignment aid for casing.

Fig. 10. Finished splice.

Fig. 11. Prototype spliced in inclined position.

Table 3. Measured Alignment on Test Specimens with Spliced BRBs					
		Alignment before Welding Core + Stiffener (in.)		Alignment after Welding Core + Stiffener but before Welding Casing Plates (in.)	
Number	ID	In-Plane	Out-of-Plane	In-Plane	Out-of-Plane
3	1902A1	<1/16	<1/16	<1/16	<1/8
4	1902A2	<1/16	<1/16	<1/8	<1/8
5	1903A	<1/16	<1/16	<1/8	<1/4

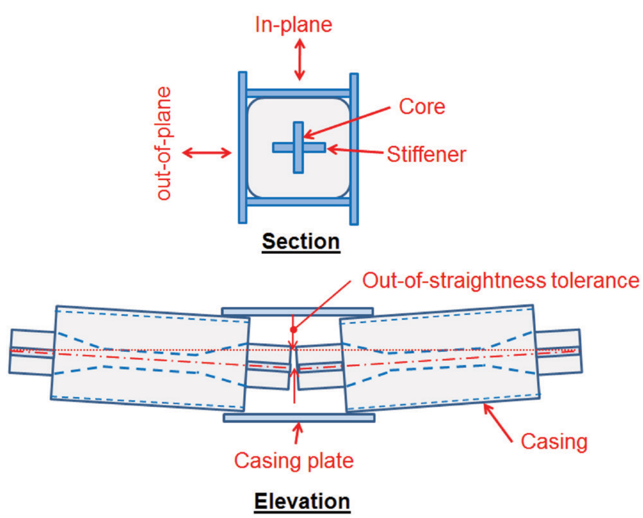

Fig. 12. Out-of-straightness tolerance.

out-of-straightness in the splice. Table 3 summarizes the tolerance measured from the spliced specimens.

BRB TESTING

The tests were conducted using the Multi-Axial Testing System (MATS) at the National Center for Research on Earthquake Engineering (NCREE), Taipei, Taiwan (Tsai et al., 2010a, 2010b). The MATS platen is capable of imposing displacements in all six degrees of freedom. For the tests, longitudinal and transverse displacements were imposed simultaneously to capture the axial and rotational demands on the specimen. One end of the specimen was attached to a concrete strong wall, while the other was attached to the MATS platen where the deformations were imposed on the specimen via horizontal and vertical actuators. Figures 13 and 14 show the test setup for the 21-ft-long braces (specimens 3 and 4). Four displacement transducers (D1 to D4 shown in Figure 13) measure the axial deformations of the brace specimen (D1 and D2) and gusset brackets (D3 and D4). The brace axial deformation, Δ_b, is taken as the average

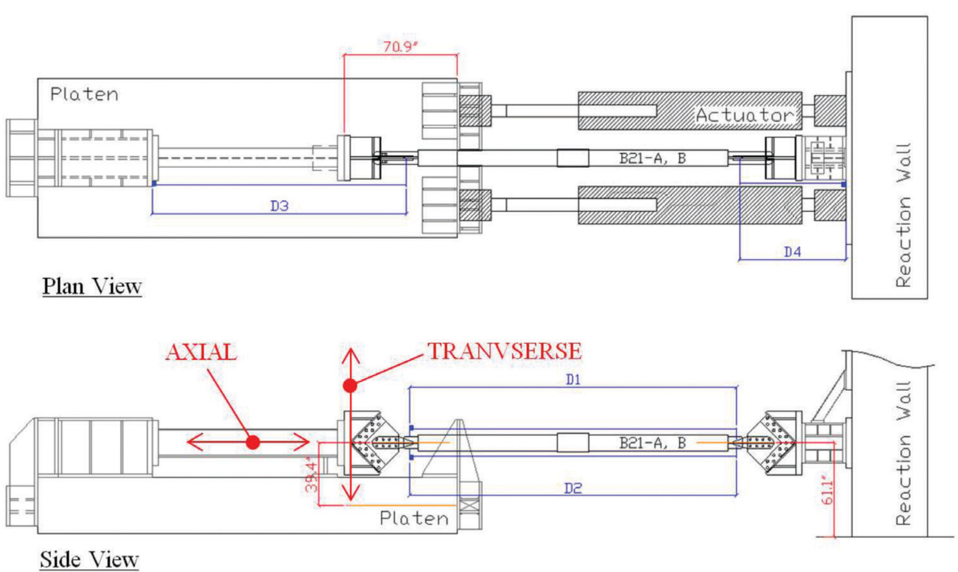

Fig. 13. Test setup.

of the displacement measured by displacement transducers D1 and D2. Transducers D3 and D4 measure the deformations of the gussets, wall bracket, platen brackets and fixtures, as well as deformations due to bolt slip. Longitudinal and transverse displacements of the platen were also recorded. The force measured by the load cell in each actuator that drove the platen was recorded. The test setup for the other braces is similar.

The BRBs were connected to gusset plates similar to those in actual construction. To reduce the cost of the testing program, as well as shorten the time between each set of tests, the gusset plates for each type of end connection were reused; that is, the same gussets for pin-end were used for both specimens 1 and 2, and the gussets for bolt-end were used for specimens 3 through 6. The gusset plates were bolted to reaction blocks, which were in turn anchored to the strong wall and platen.

DISPLACEMENT HISTORY

Subassemblage tests were performed for all six specimens. The test protocol was selected to capture the expected ductility demand of the yielding section of the steel core, obtained from the nonlinear dynamic analysis. The test protocol is defined in terms of multiples of yield displacement of the core, Δ_{by}, defined as $P_{syc}L_{ysc}/A_{sc}E$.

The parameter Δ_{by} was chosen primarily because the yielding and nonyielding length of the BRB was explicitly modeled, and the interest is in the actual ductility demand on the yielding portion of the core. The actual displacement imposed on the specimen was increased to capture the following: (1) bolt slip at the connections; (2) elastic deformation of the nonyielding section of the BRB, including the splice; and (3) elastic deformations of the gusset plates and connection fixtures. During the tests, the deformation of the platen was adjusted to ensure the amount of deformation due to bolt slip and elastic deformation of the connection fixtures were properly measured. In most cases, the actual imposed deformations on the specimen exceed that required by the protocol because the connection fixtures, bolts and so on did not move as much as anticipated.

The AISC *Seismic Provisions* (AISC 341-10) require the specimen to be tested to $2\Delta_{bm}$, where Δ_{bm} is the brace deformation corresponding to design story drift or 1% story drift, whichever is larger. Specimens 1 and 2 represent the pin-end braces connecting the building to exterior buttresses. Unlike typical braced frames that are installed between different floors of a building, these braces are horizontal, and the brace deformation is not dependent on interstory drift; rather, it is dependent on the relative displacement between the building and the exterior buttresses. Therefore, the code requirement of minimum 1% interstory drift is not relevant in this case. For these braces, the maximum deformation of the braces under BSE-2 from our computer model was used to establish Δ_{bm}.

For the braces that are installed between floors, $2\Delta_{bm}$ (governed by the code minimum of Δ_{bm} = 1%) equates to approximately $14\Delta_{by}$ for the 21-ft specimens (specimens 3 and 4), $10\Delta_{by}$ for the 31-ft spliced specimen (specimen 5) and $9\Delta_{by}$ for the 31-ft unspliced specimen (specimen 6). The differences are due to different geometry of BRBs and different yielding length of the core as a percentage of the overall length for spliced and unspliced BRBs. Studies by Fahnestock, Sause and Ricles (2006), Mayes et al. (2004), and Sabelli, Mahin and Chang (2003) have indicated that the current protocol shown in AISC 341-10 for qualification of BRBs may not be adequate to capture maximum ductility demands on the BRBs, especially under maximum

Fig. 14. Test setup.

Table 4. Project Test Protocol

Cumulative Number of Cycles	Number of Cycles at the Specified Deformation	Longitudinal Loading in Terms of Multiples of First Significant Yield of Steel Core (Δ_{by})
2	2	$1\Delta_{by}$
8	6	$2\Delta_{by}$
10	2	$3\Delta_{by}$
12	2	$6\Delta_{by}$
17	5	$2\Delta_{by}$
19	2	$9\Delta_{by}$
24	5	$2\Delta_{by}$
26	2	$13\Delta_{by}$
31	5	$2\Delta_{by}$
33	2	$15\Delta_{by}$
38	5	$2\Delta_{by}$
39	1	$18\Delta_{by}$
44	5	$2\Delta_{by}$
45	1	$21\Delta_{by}$
50	5	$2\Delta_{by}$

considered earthquakes (BSE-2 level earthquake per ASCE-41-06) for low- to mid-rise buildings. Many of the existing published tests have been limited to AISC requirements for maximum ductility. In order to study whether the BRBs can accommodate anticipated deformation under BSE-2, the braces were tested to at least $21\Delta_{by}$.

In addition, results from the nonlinear time-history analyses showed that cycles of large excursions were interspersed by cycles of relatively small displacements. For this reason, the project protocol was designed with five to six cycles of small deformations ($2\Delta_{by}$) in between two cycles of large deformations ranging from $3\Delta_{by}$ to $21\Delta_{by}$. See Table 4 for the project test protocol.

To capture concurrent axial and rotational demands on the brace, transverse displacements were applied simultaneously to the axial displacements to meet the AISC 341-10 "subassemblage" test requirements. As discussed earlier, specimens 1 and 2 are for pin-end braces connecting the building and exterior buttresses; thus, brace rotation demand is from the building horizontal displacement perpendicular to the axis of the braces. The transverse displacements were 30% of those required by axial demand. For the remaining specimens, the transverse displacements were based on the geometry of the braced frames. That is, the 21-ft BRBs (specimens 3 and 4) are intended for frames in chevron configuration with slope of 1:1 (horizontal to vertical); thus, the transverse displacements were equal to the longitudinal displacements. The 31-ft-long BRBs (specimens 5 and 6) are intended to be in single diagonal configuration with slope of 2:1; thus, the transverse displacements were 60% of the longitudinal displacements. The range of vertical displacement of the equipment was limited to ±2.5 in. and cannot accommodate both maximum positive and maximum negative transverse displacements (which exceed 4 in. at larger cycles) for the longer braces. An initial offset of 2 in. was introduced to the platen table, giving it a range of +0.5 in. and −4.5 in. to allow the required maximum transverse displacement in negative direction.

Figure 15 (page 34) shows the project testing protocol for the 21-ft-long BRBs, and Figure 16 (page 35) shows the testing protocol for the minimum criteria outlined in AISC 341-10. The total cumulative ductility demand for the project test protocol is in excess of $500\Delta_{by}$, which substantially exceeds the $200\Delta_{by}$ that is currently required by AISC 341-10. The project testing criteria are much more demanding than the AISC testing protocol in terms of number of cycles and cumulative and peak ductility.

Subsequent to the project test protocol, all specimens were tested to failure with either a high amplitude protocol or increasing amplitude protocol.

For specimens 1 and 2, the failure test was based on incrementally increasing the amplitude at each cycle until failure (see Table 5). For specimens 3, 4 and 5, we elected to study the effect of a potential aftershock with lower amplitude but a larger number of cycles. In these failure tests, the amplitude of the largest cycle was limited to $15\Delta_{by}$ and repeated until the specimen failed (see Table 6).

Table 5. High-Amplitude Protocol (Specimens 1 and 2)		
Cumulative Number of Cycles (including main test)	Number of Cycles at the Specified Deformation	Increasing Deformation Corresponding to Multiples of First Significant Yield of Steel Core (Δ_{by})
51	2	$24\Delta_{by}$
53	2	$27\Delta_{by}$
55	2	$30\Delta_{by}$
57	2	$33\Delta_{by}$
59	2	$36\Delta_{by}$
61	2	$39\Delta_{by}$

Table 6. High-Cycle Protocol (Specimens 3, 4 and 5)		
Cumulative Number of Cycles (including main test)	Number of Cycles at the Specified Deformation	Deformation Corresponding to Multiples of First Significant Yield of Steel Core (Δ_{by})
51	2	$3\Delta_{by}$
54	3	$2\Delta_{by}$
56	2	$6\Delta_{by}$
59	3	$2\Delta_{by}$
61	2	$9\Delta_{by}$
Until failure	Until failure	$15\Delta_{by}$

EXPERIMENTAL RESULTS

Specimens 1 through 5 passed the project protocol test sequence without failure. The behavior of the braces was stable and repeatable at each cycle. The steel core projection, where it exits the casing, did not show any unusual deleterious effects from the combined axial and flexural strains. No visible lateral displacement was observed for any of the specimens, including those with splices.

During the high-amplitude protocol tests, the steel cores for specimens 1 and 2 fractured in tension during the first and second cycles of the high-amplitude test, respectively. During the high-cycle protocol testing, steel cores of specimens 3, 4 and 5 fractured in tension during the seventh, third and third cycles at $15\Delta_{by}$, respectively.

Specimen 6 exhibited gusset bending and buckling during the compression cycle at $21\Delta_{by}$ during the project testing protocol. At this cycle, the brace had been subjected to cumulative inelastic deformation in excess of $730\Delta_{by}$, based on actual measured deformation. It is important to note the same gussets had been used for the previous three specimens.

For bolt-ended BRBs (specimens 3 through 6), bolt slip was observed at cycles with amplitudes exceeding $9\Delta_{by}$. The slip-critical bolts were sized for service-level loads. After the tests, we examined the bolt holes and did not observe any evidence of deformation at bolt holes.

The summary of test results, including effects of test protocol and subsequent high-amplitude or high-cycle protocol tests, for each of the six specimens is shown in Table 7.

Comparing maximum longitudinal deformation between specimens 5 and 6, the brace with splice (specimen 5) performs as well as the brace without splice (specimen 6) in terms of maximum ductility achieved in the yield length, even though the spliced specimen has a built-in imperfection—that is, out-of-straightness of ¼ in. over the length of the brace. However, because the yield length of the spliced specimen is shorter than nonspliced specimen, the corresponding drift is also lower. Nonetheless, all the spliced specimens achieved at least 3.4% interstory drift, which is well in excess of 2% drift required by AISC 341-10 and the calculated demand from the nonlinear time-history analyses.

Table 8 shows the tension strength adjustment factor (ω), and compression strength adjustment factor (β) for the specimens at peak response as well as at 2% story drift obtained from the tests.

The ω values are generally slightly lower than the value used in the nonlinear time-history analysis, whereas the β values are generally higher than that used in the analysis, especially for the bolted end specimens (specimens 3 through 6). Note that all β values are still within the AISC 341-10 limit of 1.3 at two times the design story drift, or 2%.

The plots showing the applied load versus brace

Table 7. Summary of Test Results						
Specimen Number	ID	Maximum Longitudinal Deformation for All Cycles	Corresponding Interstory Drift	Number of Cycles at High Amplitude	Number of Cycles at $15\Delta_{by}$	Cumulative Inelastic Deformation for All Cycles
1	1901A1	$22\Delta_{by}$	NA[1]	1	NA	$750\Delta_{by}$
2	1901A2	$24\Delta_{by}$	NA[1]	2	NA	$947\Delta_{by}$
3	1902A1	$23\Delta_{by}$	3.4%	NA	7	$1515\Delta_{by}$
4	1902A2	$23\Delta_{by}$	3.4%	NA	3	$1472\Delta_{by}$
5	1903A	$22\Delta_{by}$	5.1%	NA	3	$1141\Delta_{by}$
6	1904A	$22\Delta_{by}$	5.8%	NA	0[2]	$736\Delta_{by}$

Notes:
1. Horizontal braces (specimens 1 and 2) are not related to interstory drift.
2. Specimen 6 exhibited gusset bending and buckling during the last compression cycle of the project protocol.

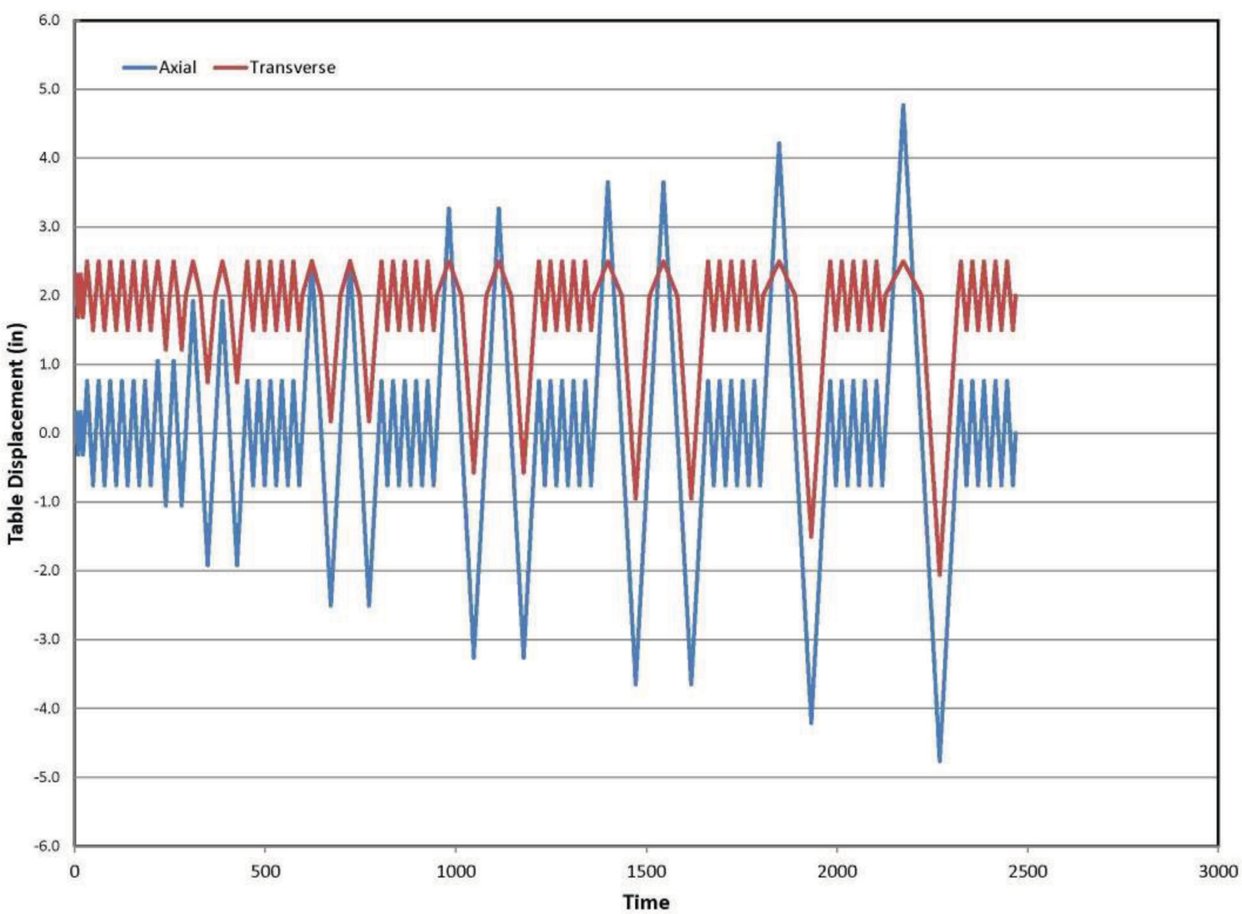

Fig. 15. Project test protocol.

Table 8. Summary of β and ω				
Specimen Number	Maximum Response Quantities for All Cycles		Maximum Response Quantities for 2% Story Drift	
	β	ω	β	ω
1	1.16	1.58	NA	NA
2	1.16	1.57	NA	NA
3	1.32	1.53	1.27	1.36
4	1.34	1.51	1.25	1.37
5	1.54	1.57	1.19	1.29
6	1.55	1.73	1.27	1.21

deformation for the specimens are shown in Figures 17 through 22. The dashed line represents the hysteresis behavior inputted into the computer model. As shown, at higher ductility levels, the computer model overestimates the tensile force and underestimates the compression force in the BRB (especially for the specimens with bolted ends) due to the ω and β values used. The computer model underestimates the hysteretic damping at higher ductility levels.

Review of the analysis results and computer models revealed that only a few BRBs in the project reached ductility levels in excess of $18\Delta_{by}$ under BSE-2 level seismic ground motions. The elongations for the majority of the

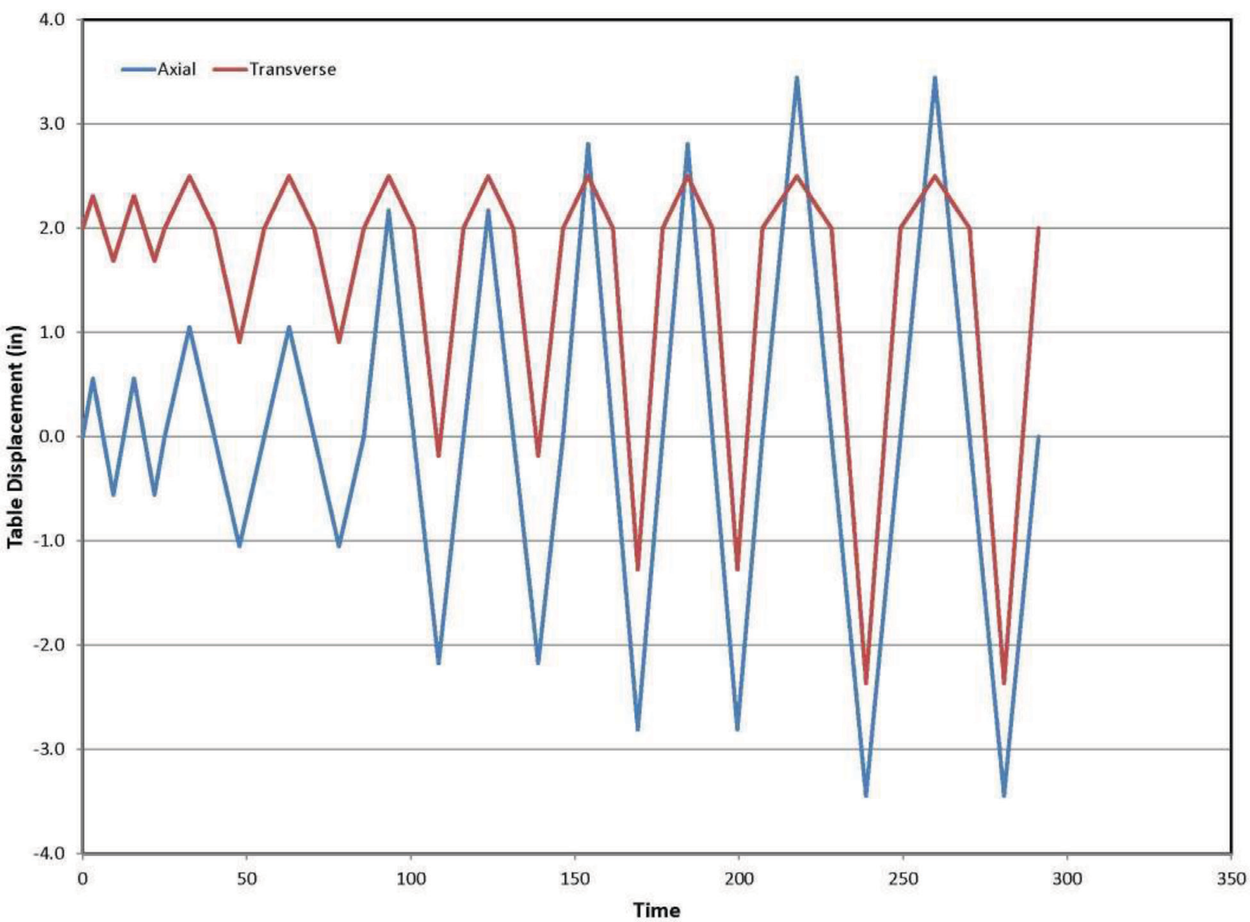

Fig. 16. AISC 341-10 test protocol.

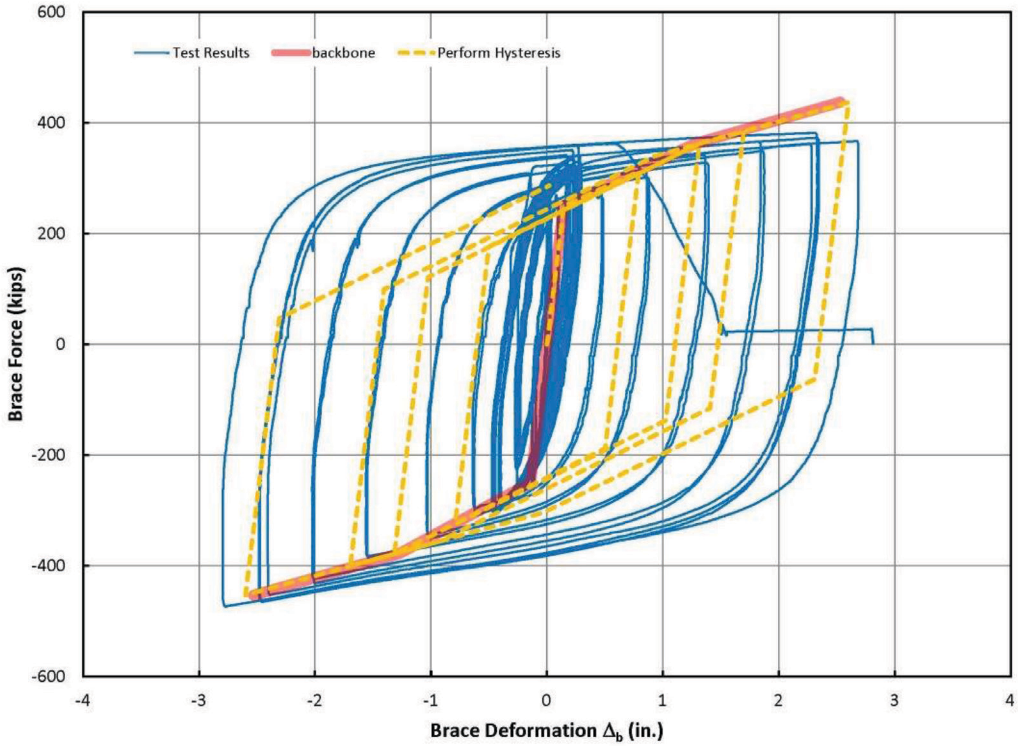

Fig. 17. Test results for specimen 1 (12-ft pinned end).

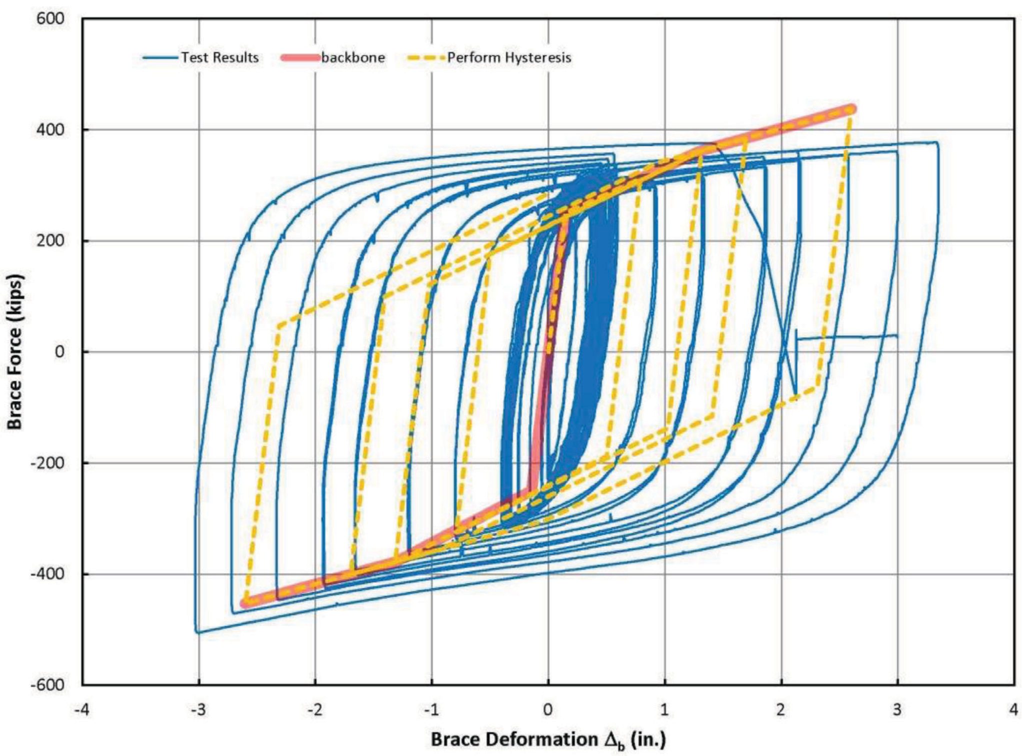

Fig. 18. Test results for specimen 2 (12-ft pinned end).

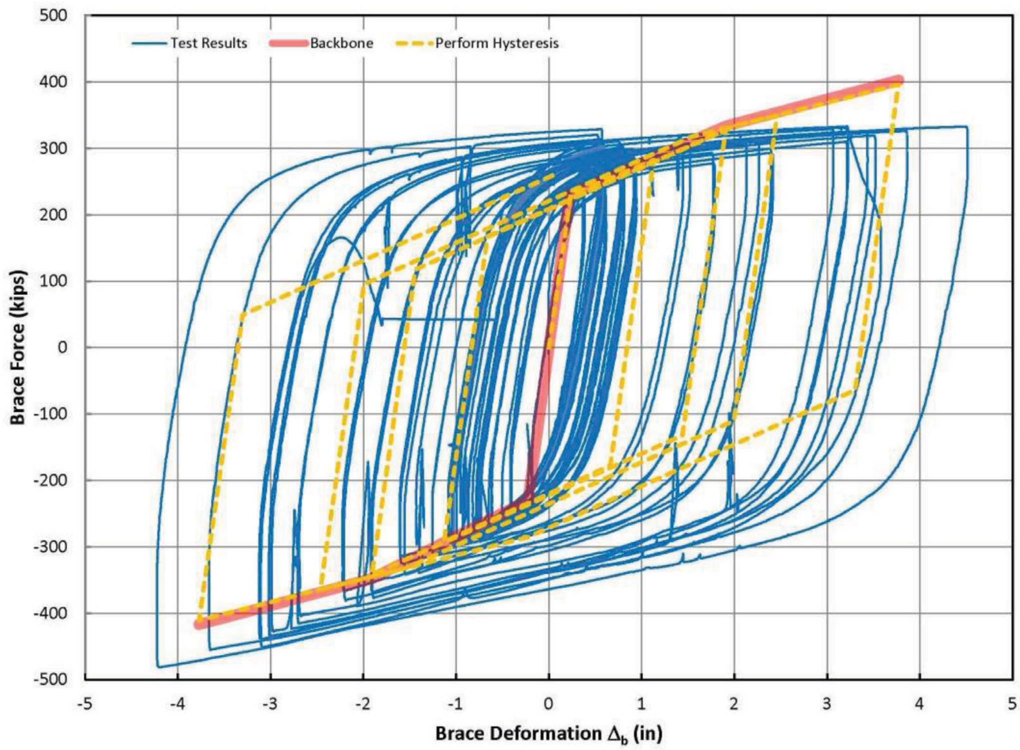

Fig. 19. Test results for specimen 3 (21-ft spliced).

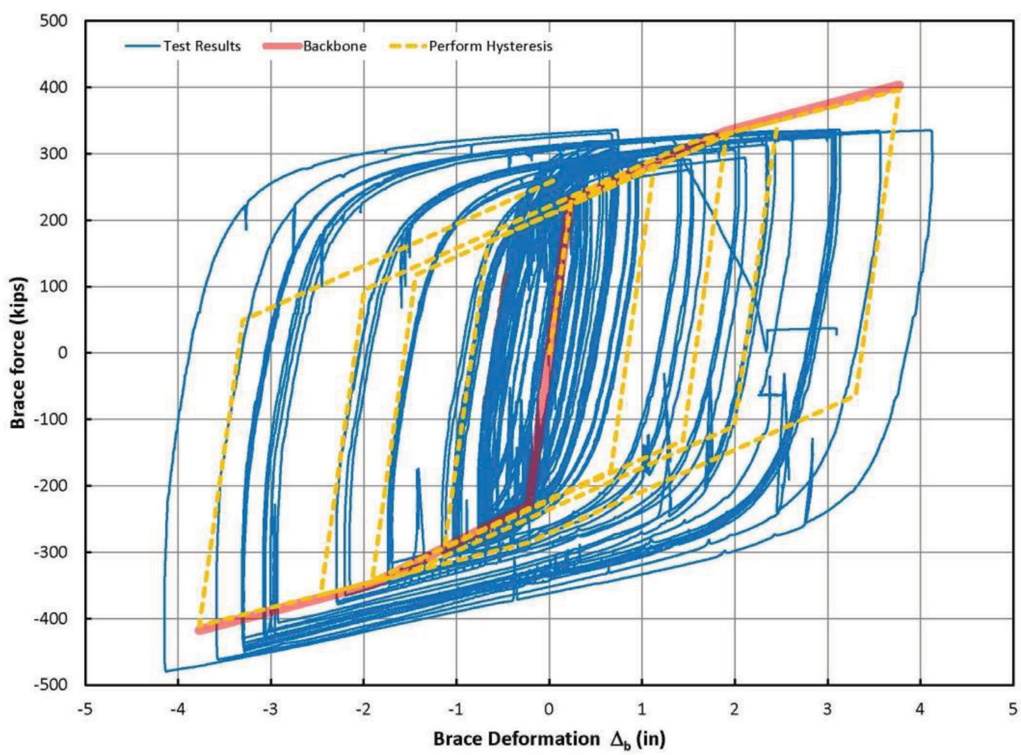

Fig. 20. Test results for specimen 4 (21-ft spliced).

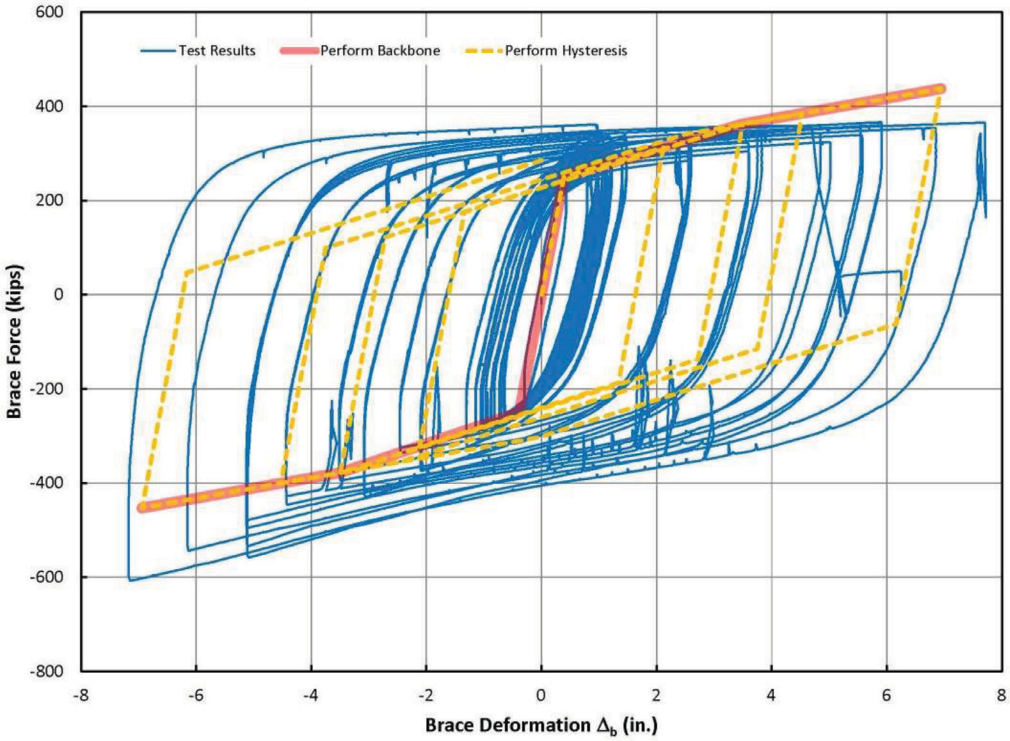

Fig. 21. Test results for specimen 5 (31-ft spliced).

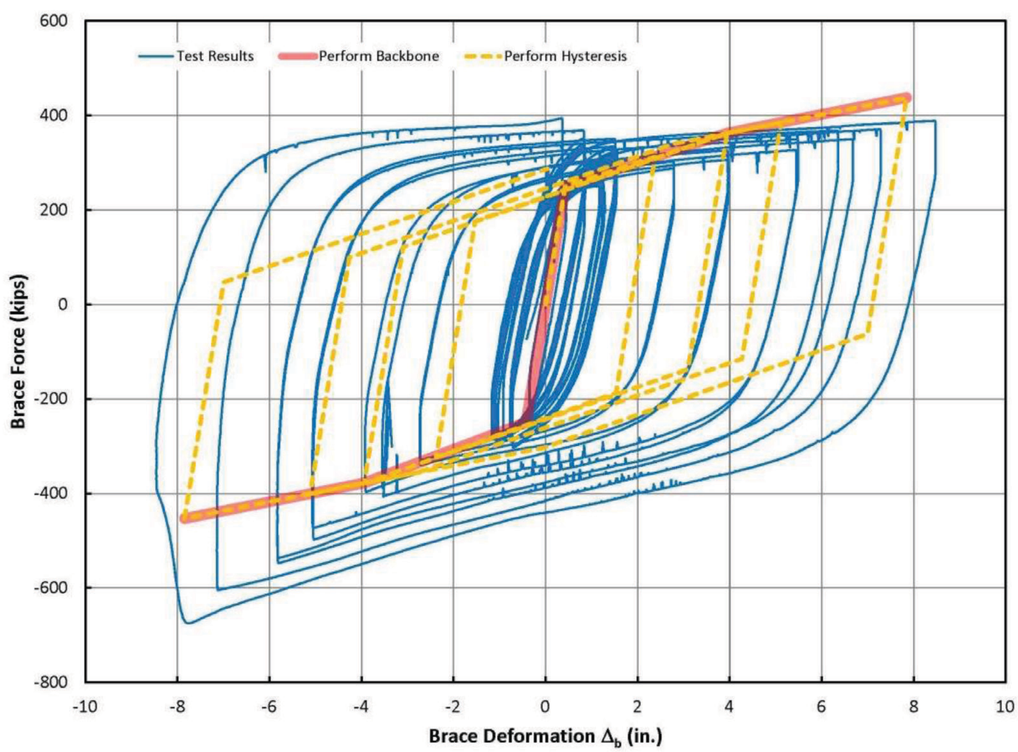

Fig. 22. Test results for specimen 6 (31-ft nonspliced).

BRBs remained within $9\Delta_{by}$. Figures 23 through 26 shows the test results for specimens 3 through 6 within brace elongations at $9\Delta_{by}$. At this ductility level, the computer model matches the tested BRB behavior very well.

Based on the results, the following conclusions and observations can be made:

- Plots showing the applied load versus brace deformations show stable, repeatable behavior.
- For all cycles within 2% of the interstory drift, the maximum compression force to maximum tension force (β) did not exceed 1.3.
- At larger drifts (i.e., ductility level), the maximum compression force to maximum tension force (β) is higher than 1.3. Further study is required to determine the cause.
- The cumulative inelastic axial deformation achieved by all specimens was significantly greater than the $200\Delta_{by}$ required by AISC 341-10.

CONSTRUCTION

The retrofit of the building started in early 2011. Congestion during construction was a major challenge. Figure 27 shows one such condition, where there were only inches between the BRB and the adjacent process lines. Nonetheless, the spliced BRBs were successfully installed without significant issue. The actual, measured, out-of-plane and out-of-straightness for each of the BRBs was well below the allowed tolerance. Aside from the scheduled 2-week shutdown period, the building was in full operation during the entire construction period.

CONCLUSIONS

Buckling restrained brace (BRB) frames have gained increasing acceptance in the structural engineering profession for seismic load-resisting systems of new and retrofit construction. A spliced BRB was developed where site conditions would not allow a standard BRB to be installed. The testing program and subsequent construction showed that the spliced BRB can be used when needed. The performance of

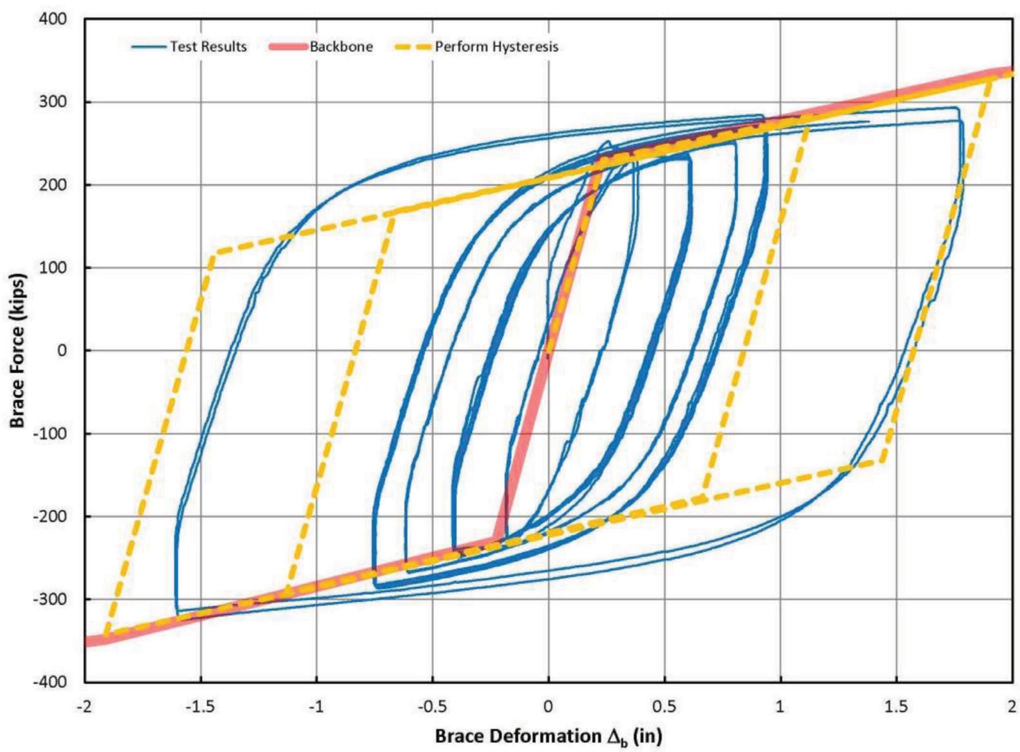

Fig. 23. Test results for specimen 3 within $9\Delta_{by}$.

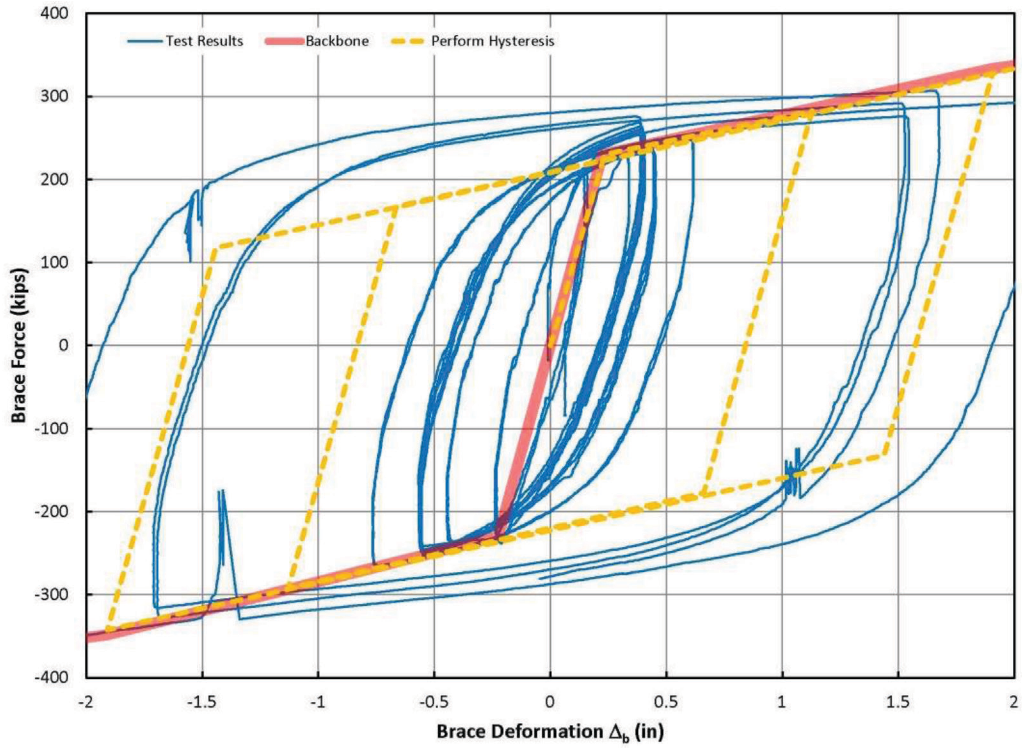

Fig. 24. Test results for specimen 4 within $9\Delta_{by}$.

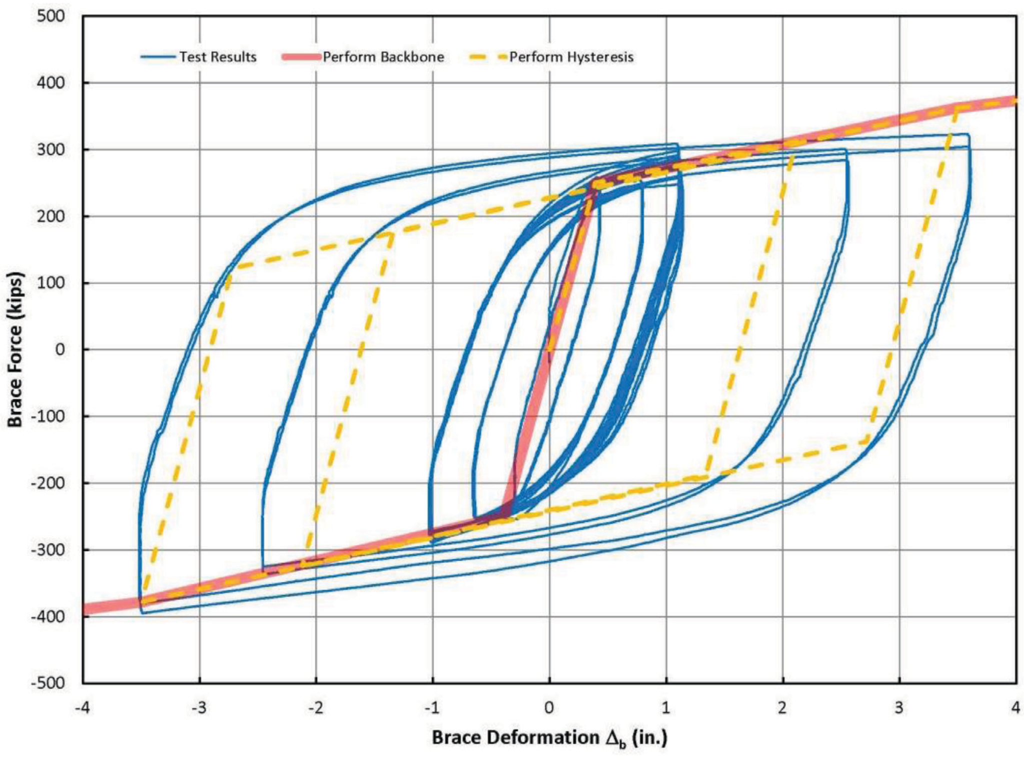

Fig. 25. Test results for specimen 5 within $9\Delta_{by}$.

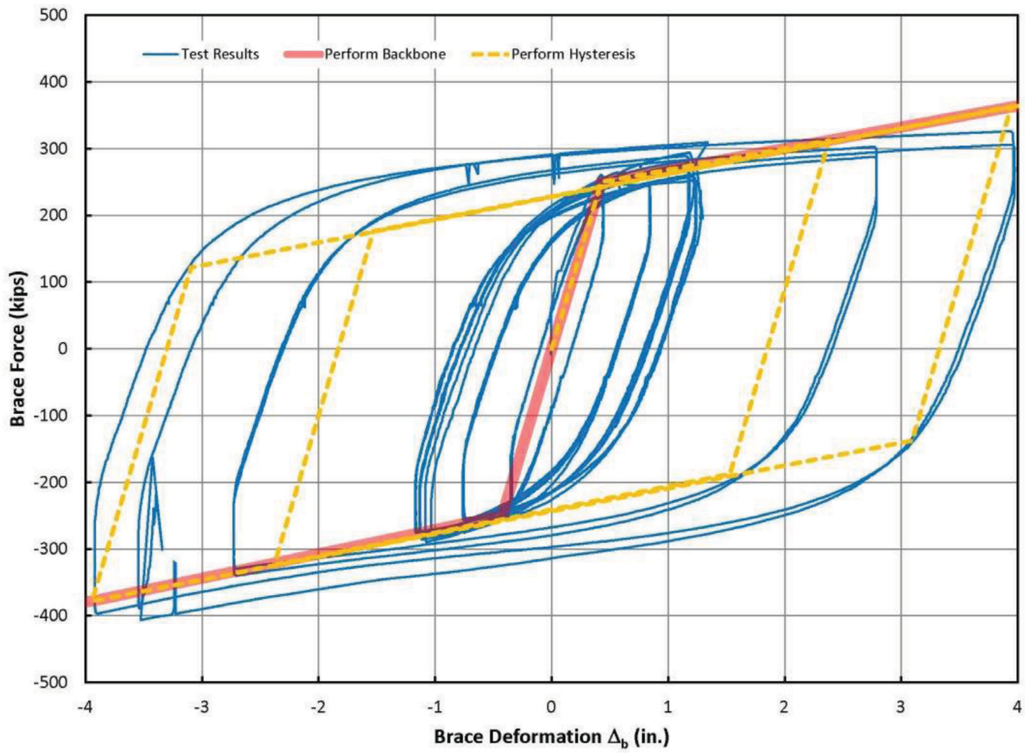

Fig. 26. Test results for specimen 6 within $9\Delta_{by}$.

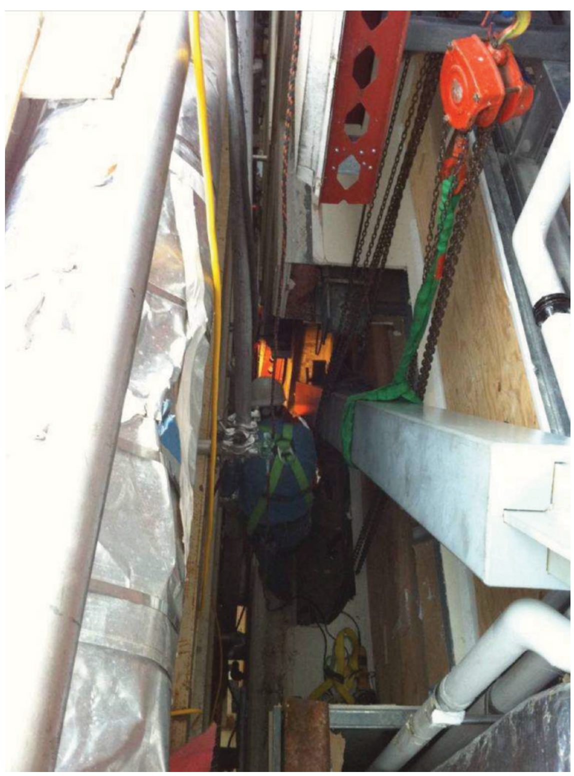

Fig. 27. Spliced BRB installation.

the spliced BRB was comparable to a standard BRB and has repeatable and expected hysteretic behavior. In fact, the testing program carried out as part of this project showed that a properly designed and detailed BRB can withstand testing that is well in excess of the current AISC 341-10 testing protocol in terms of cumulative ductility and maximum ductility demand. A prototype test program was instrumental in assessing constructability, tolerances and other potential issues prior to actual construction. In addition, preconstruction planning and close coordination among the engineer, fabricator and contractor are crucial for a successful project.

Studies by Fahnestock et al. (2006), Mayes et al. (2004) and Sabelli et al. (2003) have indicated that the current protocol shown in AISC 341-10 cyclic testing for qualification of BRBs may not be adequate to capture maximum ductility demands on the BRBs, especially under maximum considered earthquakes

ACKNOWLEDGMENTS

The project team consisted of Simpson Gumpertz and Heger, BAGG Engineers and Eichleay Engineers. The BRB suppliers, CoreBrace Inc. and the National Center for Research on Earthquake Engineering (NCREE), Taiwan, provided generous assistance in this project. Their help is gratefully acknowledged. The opinions and findings are those of the authors and do not necessarily reflect the views of individuals acknowledged herein.

REFERENCES

AISC (2010), *Seismic Provisions for Structural Steel Buildings,* AISC 341-10, American Institute of Steel Construction, Chicago, IL.

ASCE (2006), *Seismic Rehabilitation of Existing Buildings,* ASCE-41-06, American Society of Civil Engineers, Reston, VA.

Fahnestock, A.L., Sause, R. and Ricles, J.M. (2006) "Analytical and Large-Scale Experimental Studies of Earthquake-Resistant Buckling Restrained Braced Frame Systems," ATLSS Report No. 06-01, September 2006.

Mayes, R.L., Goings, C., Wassim, H., Harris, S., Lovejoy, J, Fanucci, J. P., Bystricky, P. and Hayes, J.R. (2004) "Comparative Performance of Buckling-Restraint Braces and Moment Frames," *Proc. 13th World Conference on Earthquake Engineering*, Vancouver, BC, Canada, Paper No. 2887.

Sabelli R., Mahin, S. and Chang, C. (2003). "Seismic Demands on Steel Braced Frame Buildings with Buckling Restrained Braces," *Engineering Structures*, Vol. 25, No. 5, April, pp. 655–666.

Tsai, K.C., Wei, C.Y., Wu, A.C., Lin, T.H. and Chen, J.C. (2010a), *Subassemblage Testing of Corebrace Buckling-Restrained Braces Using Pin Connection*, Report No. NCREE-02/10-01, National Center for Research on Earthquake Engineering, Taiwan.

Tsai, K.C., Wei, C.Y., Wu, A.C., Lin, T.H. and Chen, J.C. (2010b), *Subassemblage Testing of Corebrace Buckling-Restrained Braces using Bolted Connection*, Report No. NCREE-02/10-02, National Center for Research on Earthquake Engineering, Taiwan.